Inorganic Fullerenes

DOI: 10.1002/anie.200602136

Structure and Stability of Molybdenum Sulfide Fullerenes**

*Andrey N. Enyashin, Sibylle Gemming, Maya Bar-Sadan, Ronit Popovitz-Biro, Sung You Hong, Yehiam Prior, Reshef Tenne, and Gotthard Seifert**

Tungsten and molybdenum dichalcogenides have a layered structure similar to that of graphite. Hollow fullerene-like nanoparticles (inorganic fullerenes (IFs)) and nanotubes (inorganic nanotubes (INTs)) have been synthesized from these inorganic compounds.[1–3] Theoretical investigations provided a basic understanding of the electronic and mechanical properties of the INTs.[4–7]

These materials are currently being contemplated for numerous applications, in particular, as superior solid lubricants and as impact-resistant nanocomposites.[8] Bulk synthesis of the IFs normally yields quasispherical nanoparticles with at least 20 molecular layers and outer diameters of greater than 30 nm. In early work, the formation of hollow MoS_2 clusters with octahedral or tetrahedral shapes was often observed.[2,9,10] Laser ablation was used to produce MoS_2 nano-octahedra with diameters of 3–5 nm.[11]

These closed nanocages are the smallest IFs.[11,12] Herein, the small hollow nano-octahedra and the quasispherical nanoparticles (diameters larger than 30 nm) are termed (inorganic) fullerenes and fullerene-like nanoparticles, respectively. A detailed understanding of their structures and physicochemical properties is still lacking.

Structural models of single-layer fullerene-like MoS_2 nanoparticles with squarelike defects were investigated using a universal force field.[13] These results were used to model high-resolution transmission electron microscopy (HRTEM) images. The geometries of small fullerenes of different shapes were optimized using molecular mechanics, and the electronic spectra of the fullerenes were analyzed using the semiempirical extended Hückel method.[14] The electronic structures of the "ultrasmall" fullerene cages $(MX_2)_{48}$ (M = Ti, Zr, Nb, Mo, X = S; M = Fe, Ni, Cd, X = Cl) were calculated without geometry optimization by using a method based on density functional theory (DFT).[15]

Herein, the results of DFT calculations on MoS_2 fullerenes are presented. A detailed investigation of the synthesized nano-octahedra by electron microscopy allowed an instructive comparison with the predicted structures. Moreover, the calculations were extended to larger multiwalled MoS_2 nanoparticles through the use of several approximations. The calculated phase diagram of hollow MoS_2 nanoparticles could be directly compared to the experimentally observed structures. Our study focused on stoichiometric nano-octahedra. A more detailed study including nonstoichiometric nano-octahedra will follow.

As depicted in Figure 1a, there are two ways to "cut" triangular nanoplatelets from an MoS_2 monolayer. In case I, there are Mo–S bonds perpendicular to the edges of the triangle. In case II, there are Mo–S bonds parallel to the edges of the triangle. The association of these triangular fragments leads to closed stoichiometric polyhedra of octahedral shape, in which squarelike defects occur at the corners (Figure 1b). The edge lengths of the fullerenes are deter-

[*] Dr. A. N. Enyashin, Prof. Dr. G. Seifert
Physical Chemistry
Technische Universität Dresden
Bergstrasse 66b, 01062 Dresden (Germany)
Fax: (+49) 351-463-35953
E-mail: gotthard.seifert@chemie.tu-dresden.de
Dr. S. Gemming
Forschungszentrum Rossendorf
01314 Dresden (Germany)
M. Bar-Sadan, S. Y. Hong, Prof. Dr. R. Tenne
Department of Materials and Interfaces
Weizmann Institute of Science
Rehovot 76100 (Israel)
Dr. R. Popovitz-Biro
Electron Microscopy Unit
Weizmann Institute of Science
Rehovot 76100 (Israel)
Prof. Dr. Y. Prior
Department of Chemical Physics
Weizmann Institute of Science
Rehovot 76100 (Israel)

[**] This work was supported by the following agencies: the German–Israeli Foundation (GIF), the Minerva Foundation, the G. M. J. Schmidt Minerva Centre for Supramolecular Architectures, and the Israel Science Foundation.

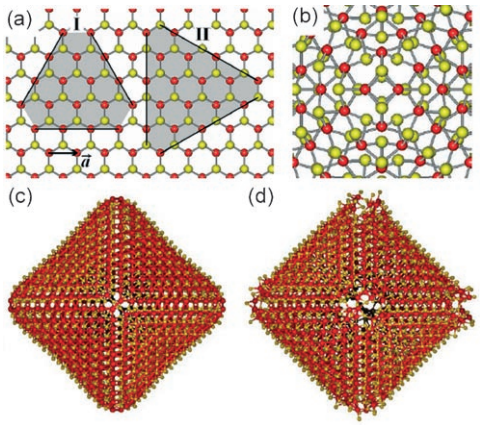

Figure 1. Structures constructed from a hexagonal MoS_2 monolayer with the lattice constant *a*: triangle faces "cut" in two possible ways (a; I and II), the ideal apex (with a squarelike defect) of a stoichiometric MoS_2 fullerene (b), the DFTB-optimized structure of an $(MoS_2)_{576}$ fullerene, which degraded to $Mo_{576}S_{1140}$ (c), and the structure of the $Mo_{576}S_{1140}$ fullerene after an MD simulation at 300 K (d). Mo red, S yellow.

mined by the number of hexagons that lie on the "cutting" edges of the triangles.

In Figure 2a, TEM images of a three-layer nano-octahedron at various tilt angles are shown. Corresponding views of the model structure are shown in Figure 2b. The agreement between the observed and the calculated structures is remarkable.

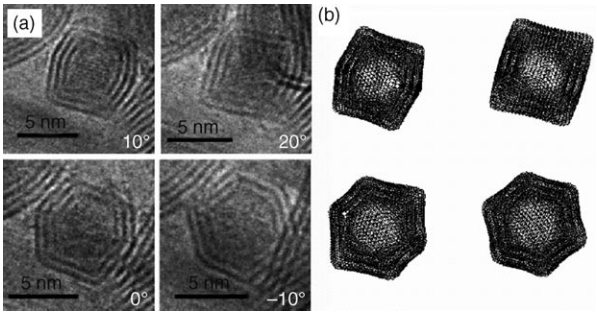

Figure 2. TEM images of a three-layer nano-octahedron at various tilt angles (a) and corresponding views of the model structure of an $(MoS_2)_{784}@(MoS_2)_{1296}@(MoS_2)_{1936}$ fullerene (b). Note the similarity between the experimentally observed and model structures.

The stoichiometric fullerenes $(MoS_2)_x$ with $x = 12$, 16, 36, 48, 64, 100, 108, 144, and 576 were investigated using the density-functional-based tight-binding (DFTB) approach (see Experimental Section). Geometry optimizations revealed that the octahedral shapes initially assigned to the small fullerenes (with $x \leq 64$) are unstable. In contrast, for the larger $(MoS_2)_x$ fullerenes (with $x \geq 100$ and diameters greater than 2 nm), the hollow octahedral structures were found to be stable. Upon optimization, the faces of the nano-octahedra remained unchanged, and only minor changes occurred along the edges. However, two sulfur atoms evaporated from each of the six corners, leading to the composition Mo_xS_{2x-12} (Figure 1c). DFTB–molecular dynamics (MD) simulations revealed considerable distortion at the corners of the initial structures, whereas the integrity of the faces and edges of the octahedron was preserved (Figure 1d). This result can be attributed to the high strain energy at the corners of the nano-octahedra. In addition, it explains the absence of small MoS_2 nano-octahedra (diameters less than 1.5 nm) in the laser-ablation product (see below).

The quantum-mechanical simulations indicated high strain at the corners of the MoS_2 nano-octahedra. The strain energy decreases with increasing size of the nano-octahedra. As a systematic investigation of the stability of fullerene-like MoS_2 nanoparticles consisting of several thousands of atoms is currently impossible using quantum-mechanical calculations, a phenomenological model for the energetics and stability the nanoparticles was developed. This model bears some similarity to one used to predict the stable structures of MoS_2 and WS_2 nanotubes, and TiO_2 nanoscrolls.[5,16]

Octahedral fullerenes are characterized by six squarelike defects (at the corners). The faces of the nano-octahedra can be represented as single-layer triangular nanoplatelets. The total energy E_f of such octahedral fullerenes can be expressed by Equation (1), where N_i, N_r, and N_p are the numbers of

$$E_f = N_i\,\varepsilon_i + N_r\,\varepsilon_r + N_p\,\varepsilon_p \tag{1}$$

molybdenum and sulfur atoms at the faces, edges, and corners, respectively. N_i and N_r are determined by the edge length of the particle (Figure 1a), and N_p is constant (36 atoms). The sum of N_i, N_r, and N_p is the total number of atoms N. ε_i, ε_r, and ε_p are the corresponding energies per atom. For multilayer fullerenes composed of k shells, the energy of the van der Waals interaction ε_{vdW} between the layers can also be considered. The total energy per atom E_t/N can then be expressed by Equation (2). The energies ε_i, ε_r, and ε_p can be

$$\frac{E_t}{N} = \frac{\varepsilon_i \sum_{j=1}^{k} \sqrt{N_j}(\sqrt{N_j}-6) + \varepsilon_r \sum_{j=1}^{k} (6\sqrt{N_j}-36) + 36\,\varepsilon_p\,k}{\sum_{j=1}^{k} N_j} + \frac{k-1}{k}\varepsilon_{vdW} \tag{2}$$

calculated by using the DFTB method, which was previously applied in calculations on single-walled MoS_2 nanotubes.[4–7] The value of ε_{vdW} was taken as twice the measured surface energy of MoS_2.[17] The difference between the numbers of atoms N_j and N_{j-1} for two shells of a multilayer nano-octahedron can be determined from the lattice constants a and c of bulk 2H-MoS_2 [Eq. (3)].

$$\sqrt{N_j} - \sqrt{N_{j-1}} = 3\sqrt{2}\frac{c}{a} \tag{3}$$

The relative stabilities of the MoS_2 nano-octahedra were compared with those of triangular MoS_2 nanoplatelets. In Figure 3, the energies per atom E_t/N of nanoplatelets and octahedral fullerenes with different numbers of layers k are plotted as a function of size N. The energies are roughly proportional to $1/N$. Single-walled MoS_2 nano-octahedra were

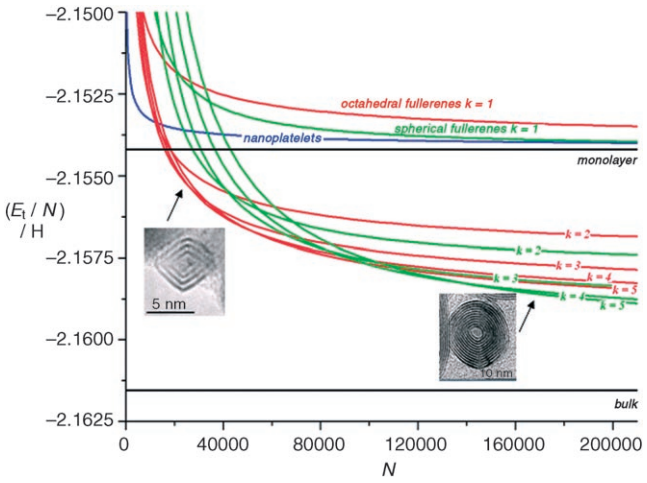

Figure 3. The dependence of the energy per atom E_t/N on the total number of atoms N for various MoS_2 nanostructures: triangular nanoplatelets, octahedral fullerenes with k shells, and spherical fullerene-like nanoparticles with k shells.

found to be less stable than nanoplatelets over the whole size range. Furthermore, the stability of the nano-octahedra increases proportionally with the number of layers. These results are consistent with published experimental data[1,2,11] and with the experimental results reported below. Indeed, single-walled octahederal nanostructures of the transition-metal dichalcogenides have not yet been observed.[11,12] Furthermore, the calculations show that multiwalled octahedral MoS_2 fullerenes with more than 12500 atoms are more stable than the corresponding nanoplatelets.

The present approach also allows the estimation of the relative stabilities of quasispherical fullerene-like MoS_2 nanoparticles (Figure 3). The results explain the experimental observation that these quasispherical nanoparticles occur in much larger sizes than the nano-octahedra. The exact nature, number, and distribution of the defects causing the spherical topology of these MoS_2 particles are not yet known. However, it can be assumed that their number is quite small compared to the total number of atoms in the nanoparticle and, thus, that the stability of the nanoparticle is mainly determined by the strain energy. The strain energy of a spherical particle is inversely proportional to the square of the sphere radius and, therefore, to the number of atoms N_j within a fullerene-like shell. Taking the van der Waals interactions between the shells into account [Eq. (2)], the energy per atom E_t/N for a spherical MoS_2 nanoparticle with k layers can be expressed by Equation (4). Considering elasticity theory,[18] the factor β can

$$\frac{E_t}{N} = \varepsilon_i + \frac{\beta k}{\sum_{j=1}^{k} N_j} + \frac{k-1}{k}\varepsilon_{vdW} \quad (4)$$

be obtained from investigations on single-walled MoS_2 nanotubes.[5] The relationship between the numbers of atoms N_j and N_{j-1} in two adjacent concentric shells is given by Equation (5).

$$\sqrt{N_j} - \sqrt{N_{j-1}} = \sqrt{\sqrt{3}\pi}\frac{c}{a} \quad (5)$$

In Figure 3, the energies per atom are calculated for hollow spherical MoS_2 nanoparticles with various values of k. Analogously to the nano-octahedra, the single-walled spherical nanoparticles are less stable than nanoplatelets over the entire range of N. The stability of the hollow spherical nanoparticles increases dramatically with the number of layers. The most important result is the crossing of the energy curves for the nano-octahedra and the nanospheres at sizes less than 100000 atoms. Thus, the present calculations reveal, in full agreement with the experimental data (see below), a peculiar dependence of the shape of MoS_2 nanoparticles on their size. Multiwalled octahedral MoS_2 fullerenes represent an intermediate allotropic form between small nanoplatelets, which are stable with hundreds to thousands of atoms, and multiwalled quasispherical fullerene-like particles, which are stable with more than 10^5 atoms (diameters greater than 30 nm).

To verify the results of the calculations, nano-octahedra were produced by the laser ablation of MoS_2 and were analyzed by TEM, HRTEM, and the associated techniques of electron diffraction (ED) and electron energy loss spectroscopy (EELS). Many of the nano-octahedra were nonperfect. For example, the angles at the corners of some of the nano-octahedra were not sharp; at least one of the visible corners was rounded. Pairs and even triplets of nano-octahedra with either a common wall (face) or edge were also observed. Thus, the TEM images confirm the theoretical prediction of high strain energy at the corners of these nanoparticles.

To compare the predicted size region of stability of the nano-octahedra to the experimental observations, we performed a quantitative analysis of the edge lengths of the nano-octahedra (using a procedure similar to that described by Parilla et al.[11]). Our results are summarized in Table 1. In

Table 1: Average edge lengths and total number of atoms for nano-octahedra produced by the laser ablation of MoS_2.

Layer	Average edge length[a]	Average number of atoms in shell[b]
4	15.8 ± 4.6	3048 (1428, 4776)
3	13.3 ± 3.5	2004 (1176, 3444)
2	9.9 ± 3.1	1176 (564, 2004)
1	6.2 ± 3.1	408 (84, 948)
Average	10.8 ± 4.4	1428 (408, 2676)

[a] In units of $a = 3.16$ Å, the lattice constant of 2H-MoS_2. Standard deviations are given. [b] The minimum and maximum number of atoms in the shell are given in parentheses.

agreement with our predictions, no single-walled fullerenes were observed: all of the nano-octahedra consisted of several layers. The largest nano-octahedra had outer shells with edge lengths of 24–25 times the a cell parameter. This length corresponds to 2300–2496 molybdenum atoms per shell (or approximately 25000 atoms (both molybednum and sulfur) in total for a five-layer nano-octahedron), which is less than the upper value of approximately 10^5 atoms calculated with our model (Figure 3). The average shell size was determined from all of the nano-octahedra investigated herein. Both theory and experiment clearly indicate the existence of a window of stability for octahedral nanoparticles.

Different types of MoS_2 samples were analyzed by EELS. The spectra recorded for plates of 2H-MoS_2 showed high signal-to-noise ratios and very distinct Mo $L_{3,2}$ and S K peaks. The S/Mo ratio was determined by integrating the S K edge relative to the Mo $L_{3,2}$ edge. The 2H-MoS_2 plates were analyzed in two configurations, with their c axis either parallel ($\| c$) or perpendicular ($\perp c$) to the beam (that is, with the $\{MoS_2\}$ sheets in the structure perpendicular or parallel to the beam). The EELS signal and, consequently, the S/Mo ratio showed a strong orientation dependence. For the $\perp c$ orientation, an average S/Mo ratio of 1.95 ± 0.2 was determined, while for the $\| c$ orientation, a ratio of 1.65 ± 0.2 was determined. For multilayer quasispherical fullerene-like nanoparticles (diameter of 50 nm),[19] an orientation-independent S/Mo ratio of 1.6 ± 0.1 was determined, which served as a reference for determining the S/Mo stoichiometry in the nano-octahedra. For the analysis of the laser-ablated samples, the illuminated area was no larger than 50 nm^2 and typically

contained two to four nano-octahedra and some amorphous material. The intensity of the S K peak was significantly reduced in the spectrum of the nano-octahedra: the S/Mo ratio of 1.3 ± 0.1 corresponds to a sulfur deficiency of approximately 35% with respect to the composition of the quasispherical fullerene-like nanoparticles. Several tests were done to confirm that no beam damage took place during the EELS analysis. The measured sulfur deficiency may also reflect a low S/Mo ratio in the amorphous material between the nano-octahedra.

Quantitative analysis of the low-energy regions of the spectra was also undertaken. The plasmonic part of the spectrum of the nano-octahedra was compared with those of the larger quasispherical fullerene-like nanoparticles and the 2H-MoS_2 plates. For the fullerene-like MoS_2 nanoparticles, the statistically averaged peak occurred at (24.6 ± 0.3) eV and its full width at half maximum was 9.8 eV; for the nano-octahedra, the peak occurred at (23.7 ± 0.4) eV and had a width of 16.9 eV. The broadening of the plasmon peak in the spectrum of the nano-octahedra can be ascribed to the large contribution from the surface plasmon near 16 eV.[19] This contribution may also be the reason for the shift of the plasmon peak to lower energy. The overall similarity between the two spectra is an indication of the close relationship between the nano-octahedra and the 2H-MoS_2 plates.

An example of an electronic density of states (DOS) curve calculated for an octahedral Mo_xS_{2x-12} nanostructure is shown in Figure 4. The DOS profiles of the fullerenes are quite similar to those of semiconducting MoS_2 nanotubes and bulk 2H-MoS_2.[4] Although the general features of the electronic structures are the same in all these cases, those of the hollow fullerenes exhibit metallic character. The gap between the highest occupied molecular orbital (HOMO) and the lowest unoccupied molecular orbital (LUMO) does not exceed a few hundredths of an electronvolt, irrespective of the size of the nano-octahedron. The valence band (−7.5 to 1.5 eV) has mixed Mo 4d and S 3p character. The states near the HOMO (Fermi energy) and the LUMO of the octahedral Mo_xS_{2x-12} fullerenes have mainly Mo 4d character.

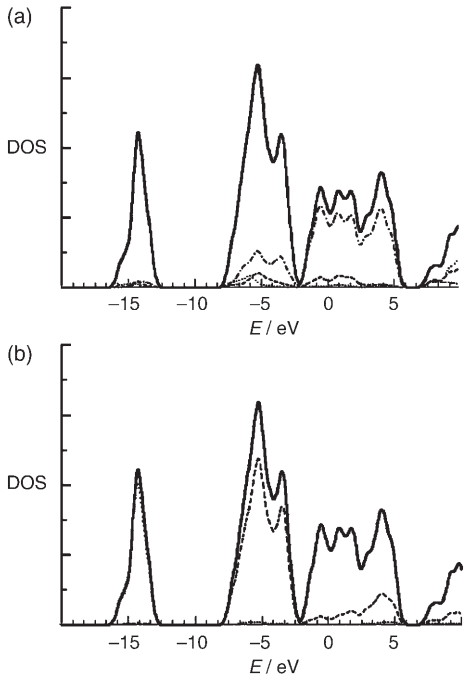

Figure 4. Molybdenum (a) and sulfur (b) DOS curves for an $Mo_{100}S_{188}$ nano-octahedron (calculated using the DFTB method). d states –•–•, p states -----, s states •••••; 0 eV corresponds to the HOMO energy (Fermi energy).

A Mulliken charge-distribution analysis reveals a charge transfer from the molybdenum to the sulfur atoms. The charges in an MoS_2 monolayer or nanotube are −0.453 and +0.906 for the sulfur and molybdenum atoms, respectively.[4] For an octahedral Mo_xS_{2x-12} fullerene (for example, $Mo_{576}S_{1140}$) average charges of −0.41 and −0.47 are calculated for the internal and external sulfur atoms, respectively, and a charge of +0.91 is calculated for the molybdenum atoms. Similar differences between the charges of the internal and external sulfur atoms were found for MoS_2 nanotubes.[4]

In summary, atomic models of molybdenum sulfide nanoparticles with fullerene-like structures were constructed. For the first time, their stabilities and electronic properties were investigated as a function of particle size using the DFTB method. Our calculations and MD simulations indicate that stoichiometric single-walled MoS_2 fullerenes with octahedral shapes and sizes of a few hundred atoms are unstable. This instability is attributed to the high strain energy at the corners of the MoS_2 nano-octahedra. Furthermore, in good agreement with the experimental data, the model calculations show that multiwalled nano-octahedra are stable in a limited size range of 10^4–10^5 atoms. Larger particles are converted into multiwalled MoS_2 nanoparticles with quasispherical shapes.

The electronic properties of the molybdenum sulfide nano-octahedra are found to be radically different those of the bulk solid. Nanoplatelets, nanotubes, and quasispherical nanoparticles of MoS_2 are semiconductors. In contrast, irrespective of their size and exact stoichiometry, all hollow octahedral molybdenum sulfide fullerenes exhibit a nearly vanishing gap between the HOMO and the LUMO, which are mainly of Mo 4d character.

The results presented herein should stimulate further experimental investigations, which will lead to the elucidation of the structure and the physical properties of the inorganic fullerenes and related nanostructures of MoS_2 and other layered compounds.

Experimental Section

All calculations were performed using the DFTB method[20] with full geometry optimization. MD simulations (constant number, volume, and temperature (NVT) ensemble) were performed for the optimized structures. The energies in Figure 3 are given in Hartree units (1 H = 27.2114 eV).

MoS_2 nano-octahedra: MoS_2 powder (Sigma Aldrich, 99.5%) was pressed into a pellet (diameter of 17 mm). The samples were heated at 450–700 °C in a quartz reactor. Laser ablation was conducted using pulses from a mildly focused frequency-doubled Nd:YAG laser (532 nm, 10 Hz, 8 ns, ca. 60 mJ per pulse, duration 20 min). The beam was scanned continuously across the pellet surface. The generated soot was flushed back downstream by flowing argon/helium gas

(760 Torr, 200 $cm^3 min^{-1}$) and was collected on a quartz substrate outside the oven.

The collected powder was sonicated in ethanol, placed on a carbon/collodion-coated copper grid, and analyzed by TEM (Philips CM-120, 120 kV). Furthermore, HRTEM (FEI Tecnai F-30, 300 kV) with an imaging filter (Gatan GIF) was used for EELS. Energy dispersive X-ray spectroscopy (EDS; EDAX Phoenix) was also used.

Received: May 29, 2006
Revised: August 16, 2006
Published online: December 12, 2006

Keywords: density functional calculations · electronic structure · fullerenes · molecular dynamics · nanoparticles

[1] R. Tenne, L. Margulis, M. Genut, G. Hodes, *Nature* **1992**, *360*, 444 – 446.
[2] L. Margulis, G. Salitra, M. Talianker, R. Tenne, *Nature* **1993**, *365*, 113 – 114.
[3] Y. Feldman, E. Wasserman, D. J. Srolovitz, R. Tenne, *Science* **1995**, *267*, 222 – 225.
[4] G. Seifert, H. Terrones, M. Terrones, G. Jungnickel, T. Frauenheim, *Phys. Rev. Lett.* **2000**, *85*, 146 – 149.
[5] G. Seifert, T. Köhler, R. Tenne, *J. Phys. Chem. B* **2002**, *106*, 2497 – 2501.
[6] I. Kaplan-Ashiri, S. R. Cohen, K. Gartsman, R. Rosentsveig, G. Seifert, R. Tenne, *J. Mater. Res.* **2004**, *19*, 454 – 459.
[7] I. Kaplan-Ashiri, S. R. Cohen, K. Gartsman, V. Ivanovskaya, T. Heine, G. Seifert, I. Wiesel, H. D. Wagner, R. Tenne, *Proc. Natl. Acad. Sci. USA* **2006**, *103*, 523 – 528.
[8] L. Rapoport, N. Fleischer, R. Tenne, *J. Mater. Chem.* **2005**, *15*, 1782 – 1788.
[9] R. Tenne, *Adv. Mater.* **1995**, *7*, 965 – 972, 989 – 995.
[10] L. Margulis, S. Iijima, R. Tenne, *Microsc. Microanal. Microstruct.* **1996**, *7*, 87 – 89.
[11] P. A. Parilla, A. C. Dillon, K. M. Jones, G. Riker, D. L. Schulz, D. S. Ginley, M. J. Heben, *Nature* **1999**, *397*, 114.
[12] P. A. Parilla, A. C. Dillon, B. A. Parkinson, K. M. Jones, J. Alleman, G. Riker, D. S. Ginley, M. J. Heben, *J. Phys. Chem. B* **2004**, *108*, 6197 – 6207.
[13] J. A. Ascencio, M. Perez-Alvarez, L. M. Molina, P. Santiago, M. José-Yacaman, *Surf. Sci.* **2003**, *526*, 243 – 247.
[14] A. N. Enyashin, V. V. Ivanovskaya, Yu. N. Makurin, A. L. Ivanovskii, *Inorg. Mater.* **2004**, *40*, 395 – 399.
[15] A. N. Enyashin, A. L. Ivanovskii, *Russ. J. Phys. Chem.* **2005**, *79*, 1081 – 1086.
[16] A. N. Enyashin, G. Seifert, *Phys. Status Solidi B* **2005**, *242*, 1361 – 1370.
[17] J. D. Fuhr, J. O. Sofo, A. Saul, *Phys. Rev. B* **1999**, 60, 8343 – 8347.
[18] D. J. Srolovitz, S. A. Safran, M. Homyonfer, R. Tenne, *Phys. Rev. Lett.* **1995**, *74*, 1779 – 1782.
[19] H. Cohen, T. Maniv, R. Tenne, Y. Rosenfeld Hacohen, O. Stephan, C. Colliex, *Phys. Rev. Lett.* **1998**, *80*, 782 – 785.
[20] D. Porezag, T. Frauenheim, T. Köhler, G. Seifert, R. Kashner, *Phys. Rev. B* **1995**, 51, 12947 – 12957.

